



Dark mode tailored electromagnetically induced transparency in terahertz metamaterials

Kailong Jin¹ · Xiaona Yan¹ · Xiaoyan Wang¹ · Wenjie Zhang¹ · Zuanming Jin¹ · Ye Dai¹ · Guohong Ma¹ · Jianquan Yao²

Received: 10 September 2018 / Accepted: 17 March 2019 / Published online: 3 April 2019
© Springer-Verlag GmbH Germany, part of Springer Nature 2019

Abstract

In this paper, a novel terahertz metamaterial structure composed of a pair of sub-wavelength reverse U-shaped split ring resonators (RUSRs) and cut wire (CW) resonator is designed to realize electromagnetically induced transparency (EIT) effect in weak coupling region. Theoretical and simulated results show that by modulating the relative coupling distance between CW and SRR or mutual distance between SRR pair, the EIT-like phenomenon can be tailored. Furthermore, by introducing photosensitive silicon (Si) cell into the units of the dark mode resonator, actively optical control of the EIT-like effect is realized through increasing the dark mode damping rate. The present work provides an alternative method to design ultrasensitive sensors, filters and slow-light devices in the THz regime.

1 Introduction

Due to the potential applications in high-speed telecommunications, material analysis, bio-medical technology, and security, etc., terahertz (THz) science and technology have made a dramatic development in recent years [1–4]. On the other hand, THz technology still suffers from a deficiency in efficient detectors, high-power sources, and functional devices due to the lack of materials that naturally respond well to THz radiation. Electromagnetically induced transparency (EIT) is a typical quantum interference phenomenon occurring in multiple-level (three or four levels) atomic systems, where the interference modifies the optical response of an atomic medium, resulting in a narrow transparency window within a broad absorption spectrum [5]. However, in an atomic system, implementation of the EIT needs special experimental conditions such as extremely freezing temperature and ultrahigh intensity laser, which significantly constrains its further applications. In 2008, Zhang

et al. proposed a concept of plasmon-induced transparency (PIT) by metamaterials [6], after that, a variety of metamaterial structures have been designed to mimic EIT effect. The metamaterial is a kind of artificial structure, which has some peculiar properties that natural materials do not have. Owing to its well-controlling property of incident electromagnetic waves, it has been extensively investigated to realize negative refractive index [7–10], invisibility Cloak [11, 12] and perfect lens [13], etc. Most EIT-like metamaterials are based on two kinds of resonant modes, bright mode and dark mode or super-radiation mode and sub-radiation mode. Bright mode or super-radiation mode is used to strongly couple with the incident electromagnetic wave, while the sub-radiation mode or dark mode is weakly excited or could not be excited by the incident wave directly, but by the super-radiation mode or bright mode. And the EIT-like phenomenon could be emulated in metamaterials via destructive interference between the bright mode and the dark mode, or between super-radiation mode and sub-radiation mode. To make EIT-like phenomenon occurring in a metamaterial, the two modes should have similar resonant frequency and very different Q -factor [14]. Most studied EIT metamaterials are based on cut wire (CW) and splitting ring resonators (SRRs). The CW supports a typical local surface plasma (LSP) resonance and the SRR is a well-known LC resonance of inductor and capacitor [15]. Some other typical metamaterial structures, such as fishing net structure [16], coupled waveguide resonator [17] and dipole-coupled quadrupole [18, 19], etc., were also proposed to achieve EIT phenomena.

✉ Xiaona Yan
xnyan@staff.shu.edu.cn

✉ Guohong Ma
ghma@staff.shu.edu.cn

¹ Department of Physics, Shanghai University, Shanghai 200444, China

² Institute of Laser and Opto-electronics, College of Precision Instrument and Opto-electronics Engineering, Tianjin University, Tianjin 300072, China

For practical application, it is highly desirable that the transparent window of EIT phenomena can be modulated at will. The corresponding modulated methods include passive modulation and active modulation [20–24]. The passive modulation is realized by varying geometrical parameters of the resonator structure, and the structure should be re-fabricated in each modulation, which limits its practical application. The active modulation is a real-time control of the transparent window, which can be realized with external fields, such as thermal modulation [25, 26], optical pump modulation [22, 27] or dc electric field modulation [28–33], and so on. The EIT-like transmission has perspective applications on designing slow-light devices [34, 35] and highly sensitive sensors [36].

In this paper, we design a novel metamaterial structure in THz range to realize the modulated EIT-like effect. Numerical simulation and theoretical analysis confirm that the modulation can not only be realized by modifying the separation of CW and SRRs or the separation of SRR pair, but also be realized by actively controlling damping rate of the dark mode under photoexcitation. Our work provides an alternative scheme for designing novel chip-scale ultrafast devices that would find utilities in slow-light devices, optical switch and THz active and/or passive filtering.

2 Metamaterial design and EIT effect simulation

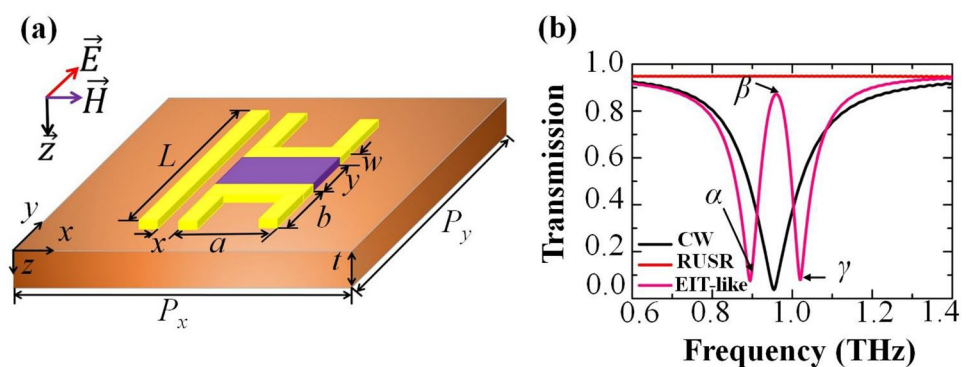
The particular unit cell of EIT-like metamaterial structure is shown schematically in Fig. 1a. The unit cell is composed of a CW resonator and a pair of reverse U-shaped split ring resonators (RUSRs), which is designed on the top of quartz substrate. The quartz substrate is a loss-free material with relative permittivity of $\epsilon_{\text{quartz}} = 3.75$. A 500 nm thick copper with a DC conductivity of $\sigma_{\text{dc}} = 5.96 \times 10^7$ S/m is chosen for fabrication of metamaterial structure [37]. The geometric parameters of one unit cell of the metamaterial structure are: length and width of the CW are $L = 95 \mu\text{m}$ and $w = 5 \mu\text{m}$, respectively. Parameters of RUSR are $a = 50 \mu\text{m}$, $b = 30 \mu\text{m}$,

$w = 5 \mu\text{m}$; periodicity of the unit cells along x - (P_x) and y -direction (P_y) are $160 \mu\text{m}$ and $120 \mu\text{m}$, respectively. The thickness of quartz substrate is $t = 20 \mu\text{m}$. The specific ‘ x ’ and ‘ y ’ represent the separation between CW and RUSR, and between two reverse U-shaped SRRs, respectively. The THz pulse is incident normally to the plane of the structure with the electric field polarized along the y -direction, and the transmission signal is collected near the output plane of the structure. The simulated results are obtained using the commercial software-CST Microwave Studio. During the numerical simulations, all boundaries of the computation volume are terminated with perfectly matched layers (PMLs) to avoid parasitic unphysical reflections around the structure. A hexahedral mesh with accuracy of 100 nm is used to make our simulation results convergent.

Figure 1b shows individual transmission profile of incident THz wave polarized along y -direction for the sole-CW (black), sole-RU-SRR (red) and the composite metamaterial structure (Pink). The CW strip couples strongly with the incident light, acting as the bright mode. The RUSR does not couple with the incident light, acting as the dark mode. The two resonators are designed to have similar resonant frequency $\beta = 0.96$ THz. Q -factor is defined as the center frequency ω_0 divided by bandwidth of the full width at half maximum $\Delta\omega$ ($Q = \omega_0/\Delta\omega$), we find that the CW possess wide spectral bandwidth with low Q -factor ($Q = 7.8$), and the RUSR has narrow spectral bandwidth (not shown here) with high Q -factor ($Q = 21.3$). The large different Q -factors of the two modes make a sharp transparency window emerge on the transmission spectrum, as shown in Fig. 1b with pink curve, where two dips occur at $\alpha = 0.89$ THz and $\gamma = 1.02$ THz, respectively.

To elucidate the coupling between the bright and dark modes, we further calculate the distributions of x -component of electric field, z -component of magnetic field, as well as surface current at three resonant frequencies, as shown in Fig. 2. At two dips $\alpha = 0.89$ THz and $\gamma = 1.02$ THz, as shown in Fig. 2a, c, d and f, the coupling between bright and dark modes is very weak. Furthermore, it is seen that the surface currents shown in Fig. 2g, i are in parallel and anti-parallel

Fig. 1 Microstructure design and simulated transmission spectra. **a** Schematic of the unit cell. The geometric parameters are: $L = 95 \mu\text{m}$, $a = 50 \mu\text{m}$, $b = 30 \mu\text{m}$, $w = 5 \mu\text{m}$, $x = 5 \mu\text{m}$, $y = 35 \mu\text{m}$. **b** Simulated transmission profile versus frequency for the sole-CW (black), RUSR (red) and the EIT-like metamaterial (pink)



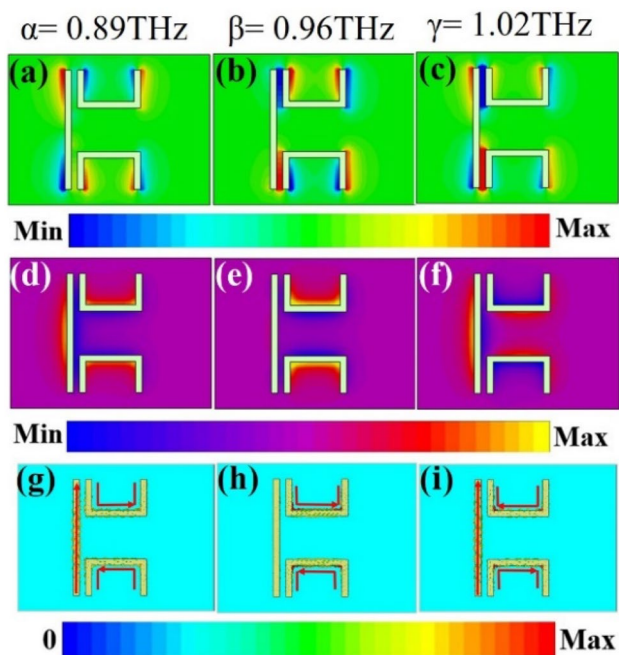


Fig. 2 Distributions of x -component of electric field (a–c), z -component of magnetic field (d–f), and surface current (red arrow represents the current direction) (g–i) at frequencies of low dip $\alpha=0.89$ THz, transparency window $\beta=0.96$ THz, and high dip $\gamma=1.02$ THz

states, respectively. For the transparent window at frequency $\beta=0.96$ THz, Fig. 2b, e and h clearly shows that the bright mode has been suppressed significantly, while the dark modes are being excited, this is a typical sign of the destructive interference between the bright and dark resonators [38], which indicates that our proposed structure can be used to realize EIT-like effect.

Next, we study the modulation of the THz transmission based on the proposed metamaterial structure. To confirm our results, both theoretical analysis and numerical simulation are performed. The theoretical analysis is based on the coupled Lorentz oscillator model, which has been widely used to analyze the coupling between the bright and dark modes, and explore the physical origin of the EIT modulations. In this model, the oscillations of bright and dark modes can be expressed as [6]:

$$\begin{pmatrix} a_1 \\ a_2 \end{pmatrix} = - \begin{pmatrix} -\omega_1 + i\gamma_1 + \omega & \kappa \\ \kappa & -\omega_2 + i\gamma_2 + \omega \end{pmatrix}^{-1} \begin{pmatrix} gE_0 \\ 0 \end{pmatrix}, \tag{1}$$

where a_1 and a_2 , γ_1 and γ_2 , ω_1 and ω_2 are the amplitudes, damping rates and resonance frequencies of the bright and dark modes, respectively. $|\omega_1 - \omega_2| = \delta$ is the resonance detuning parameter; κ is coupling coefficient between two modes; g is a geometric parameter describing the coupling strength between the bright mode and the incident THz wave. By solving Eq. (1), we obtain:

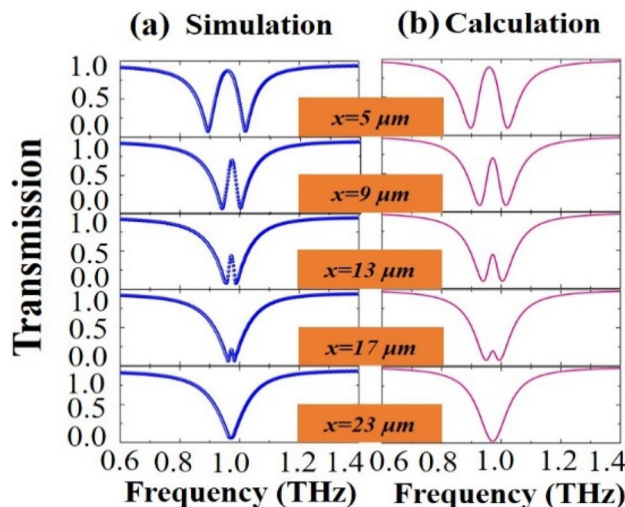


Fig. 3 The transmission spectra under various separation of CW and SRR. **a** Simulated results and **b** calculation results

$$a_1 = \frac{g(\omega - \omega_2 + i\gamma_2)E}{\kappa^2 - (\omega - \omega_1 + i\gamma_1)(\omega - \omega_2 + i\gamma_2)}. \tag{2}$$

Then, the transmission spectrum of the EIT-like metamaterial can be acquired [29]:

$$T(\omega) = 1 - |a_1/E|^2. \tag{3}$$

3 The separation dependence of EIT transmission

The modulation of THz transmission can be achieved by modifying the geometrical parameters of the metamaterial structure. It is known that the EIT-like effect results from the coupling and destructive interference between the bright and dark modes, when coupling distances changes, the coupling strength will change correspondingly, so that the EIT-like effect will be modulated. In the following, we will discuss the influences of the separations of the CW and SSR as well as the separation of SSR pair on the EIT-like effect.

Figure 3a shows that the transmission property of the EIT metamaterial can be dramatically modulated by the x value with $y=35 \mu\text{m}$ is fixed. Moreover, the simulated results exhibit very good agreement with the theoretical results (Fig. 3b). The EIT peak appears clearly with $x=5 \mu\text{m}$. As x is increased from 5 to 23 μm , the EIT peak decreases gradually. When x is larger than 23 μm , the EIT peak vanishes completely, and only a broad LSP resonance dip is observed, which demonstrates on-to-off of EIT peak modulation with changing the separation of CW and SRR.

To clarify the influence of separation x of CW and SRR on the EIT effect, we simulated the electric field and magnetic field distributions with different x values, which is presented in Fig. 4. It is seen when x is $5 \mu\text{m}$, the electric field and magnetic field are mainly localized in dark mode, which indicates that the field of the CW bright mode completely couples to that of the dark mode. By increasing x value from 5 to $23 \mu\text{m}$, the coupling between bright and dark modes decreases gradually. When x approaches $23 \mu\text{m}$, the coupling vanishes completely; as a result, the transparency window disappears.

From above discussions, it is seen that the value of x has significant influence on the coupling of electric and magnetic fields between the bright and dark modes. To verify this assertion, we employ Eq. (3) to fit the simulated curves shown in Fig. 3a, the fitting parameters with respect to x is plotted in Fig. 4k. It is seen that γ_1 , γ_2 and δ remain almost unchanged, while the coupling coefficient κ between the two modes decreases with the increases of x . Thus, it can be concluded that the modulation of EIT effect arises from weakening of the coupling strength between the bright and dark modes. As the EIT phenomenon results from destructive interference of the two modes, when the amplitude of the dark mode decreases, the interference effect will decrease accordingly. When the coupling distance, x , is increased up to $23 \mu\text{m}$, the coupling is so weak that the amplitude of the dark mode is close to zero; as a result, the EIT resonance peak vanishes completely.

There is another way to modulate EIT-like effect by shifting two U-shaped SRRs of dark mode symmetrically along y -direction. The simulated and theoretical results are presented in Fig. 5a, b, it is seen that simulation and theoretical results show very good agreement when y changes from 3 to $35 \mu\text{m}$ with fixing x at $5 \mu\text{m}$. When y is $35 \mu\text{m}$, the two SRRs are far away from each other, the transmission amplitude is the largest and the transmission line-shape is symmetric. By decreasing the distance of y , the THz transmission amplitude decreases, and the frequency detuning increases, we come closer to the typical Fano regime with an asymmetric

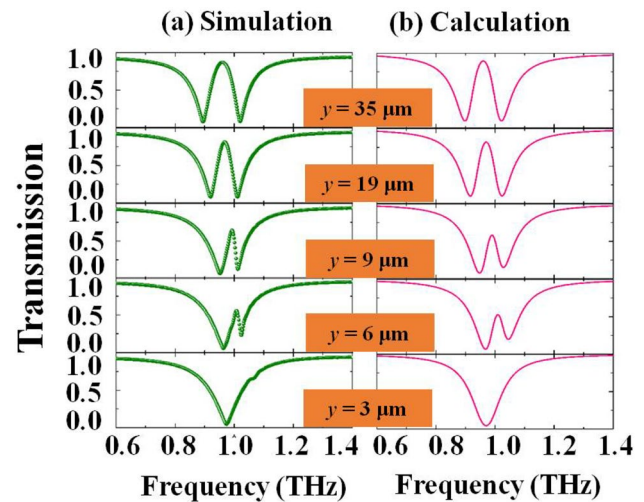


Fig. 5 Modulation of the transparency window when coupling distance between the U-shaped SRRs pair changes from 3 to $35 \mu\text{m}$, **a** simulation results and **b** calculation results

transmission line-shape that sits at the flank of the bright resonance. With y reduced to $3 \mu\text{m}$, the transparent window vanishes completely.

To better understand the physical mechanism of the mode coupling, we use coupling current model to analyze the curves shown in Fig. 5 with two examples for $y = 35$ and $3 \mu\text{m}$, respectively, which is given in Fig. 6a. When ' $y = 35 \mu\text{m}$ ', the incident THz wave is strongly coupled with the CW, through near field coupling (here the coupling occurs mainly via electric field coupling because the electric field is the strongest while the magnetic field is the weakest around two ends of the CW), the dark mode is being excited, and the current in the dark mode is induced. As a result, the electric and magnetic fields in the bright mode are suppressed, while those of the dark mode are activated, and a transparency window appears. When ' $y = 3 \mu\text{m}$ ', the dark mode is mainly excited by the magnetic field of the bright mode, the induced current direction is the same as

Fig. 4 The separation between CW and SRR, x dependence of filed distributions: **a–e** x -component of electric field distribution, **f–j** z -component of magnetic field distribution. **k** The theoretical fitting parameters under different separation value of x

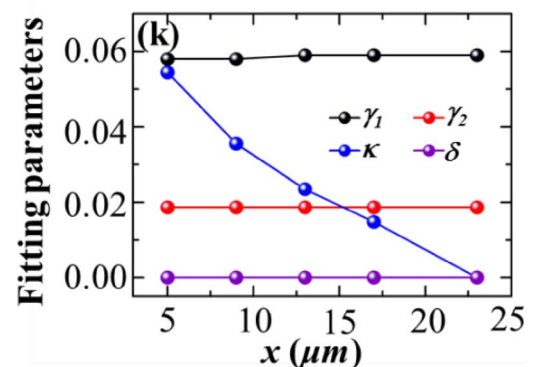
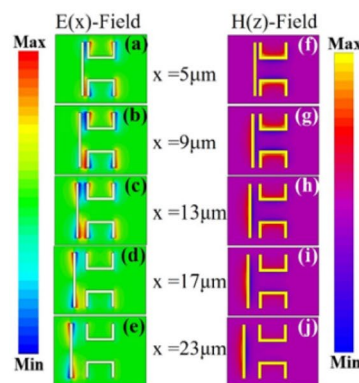
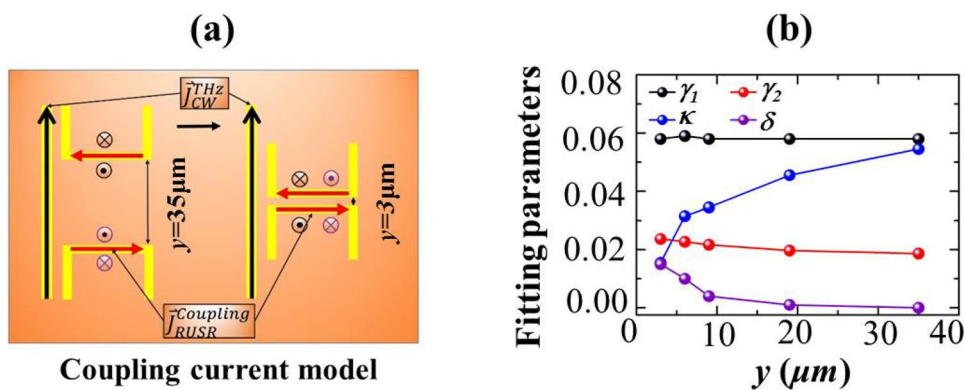


Fig. 6 a Schematics of coupling current model; **b** fitting parameters with ‘y’ value varying from 35 to 3 μm (⊗ and ⊙ represents the directions of the induced magnetic field normal to paper inward and outward, respectively)



the one of ‘ $y = 35 \mu\text{m}$ ’. However, it is seen from Fig. 5 that the transparency window disappears at this condition. The reason is that with ‘ $y = 3 \mu\text{m}$ ’, the two U-shaped resonators are close with each other, and the induced magnetic fields arising from the currents of the two U-shaped resonators suppress mutually, as a result, the induced magnetic fields will cancel each other, which leads to the disappearance of EIT-like phenomenon. When the ‘y’ value change in the range from 3 to 35 μm , as the degree of mutual inhibition of the coupled magnetic fields in the two resonators varies with the distance of y, the amplitude of the EIT-like phenomenon is varied accordingly. Figure 6b shows the fitting parameters with respect to the value of y. It is seen that when y equals 6 and 9 μm , the detuning parameter δ is quite large, and in this case, the coupling as be assigned as Fano resonance [39], so that the Fano asymmetric line-shape is observed in Fig. 5.

4 Active modulation of EIT-like effect with optical pumping

By fabricating a photosensitive silicon (Si) cell (purple area) between reverse U-shaped resonators as shown in Fig. 1a, an active modulation of the EIT resonance can be achieved with photoexcitation.

Optical illumination can modify the silicon conductivity significantly; therefore, active modulation of the EIT effect can be realized with laser irradiation on the hybrid metamaterial. Figure 7a shows the simulated transparency window with respect to the conductivity of the Si cell in the range from 0 to 15,000 S/m. Figure 7b shows the theoretical calculation of the active modulation based on Eq. (3), which shows good agreement with the simulated results.

The fitting parameters with respect to Si conductivity are plotted in Fig. 8a. It is seen that the parameters, κ , γ_1 and δ , change very little with the Si cell conductivity, while the damping rate of the dark mode γ_2 is strongly correlated with it. Thus, it can be concluded that the active modulation of EIT resonance arises from the change of the damping rate

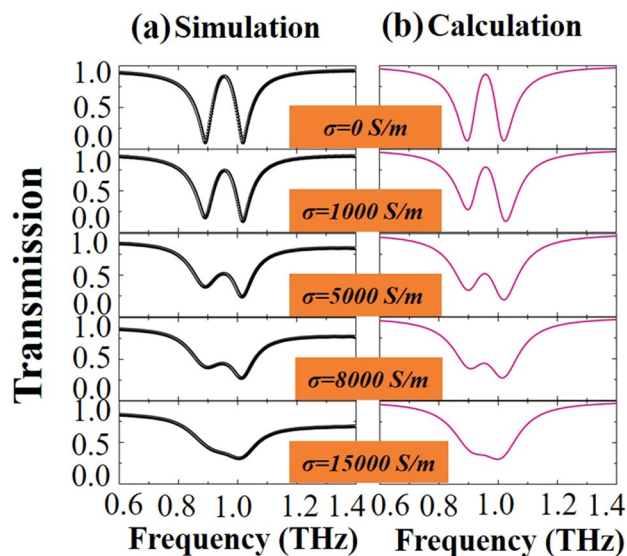
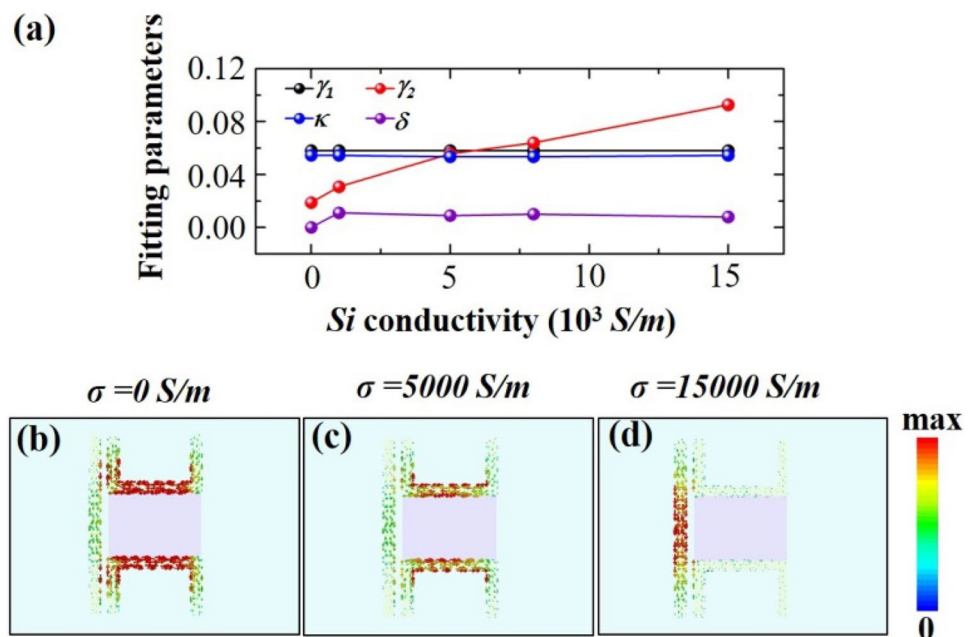


Fig. 7 Transmission spectra at different silicon conductivity ($\sigma_{\text{Si}} = 0, 1000, 5000, 8000, 15000 \text{ S/m}$). **a** Simulation; **b** theoretical calculation

of the dark mode due to the alternation of conductivity of the Si cell. Without pump light, the Si conductivity is very low. In this case, the two U-shaped SRRs are electrically isolated and the structure has small damping, thus the induced electric current primarily flow around two individual SRRs, whereas the electric current in the CW is completely suppressed, which leads to the appearance of EIT effect. With the increase of the fluence of pumping light, the conductivity in Si cell increases as well, and the two U-shaped SRRs are gradually electrically conducted. As the electric current in the two U-shaped SRRs are anti-parallel, they will suppress each other, resulting in a redistribution of the current, as shown in Fig. 8c. Furthermore, when the conductivity of Si cell increases to a certain value, the currents in two SRRs are completely suppressed, and the damping rate of the two SRRs is very larger, as a result, the current will be localized around the CW, and EIT phenomenon disappears completely under this condition.

Fig. 8 **a** The fitting parameters are plotted with respect to Si conductivity; **b–d** the surface current of the structure with silicon conductivity of 0 S/m, 5000 S/m and 15,000 S/m



5 Conclusion

In summary, a planar metamaterial structure is designed to achieve the EIT-like effect at THz frequencies. Theoretical analysis based on the coupled Lorentz oscillation model and numerical simulation verifies that the transparency window of the EIT-like effect can be modulated. The separation of CW and SRR or the SRR pair can affect the coupling strength between bright and dark modes significantly, thus the amplitude and transparency window can be modulated. Optical radiation can modify the conductivity of the integrated Si cell, thus modify damping rate of the dark mode, which can realize active modulation of the EIT-like effect. The proposed structure can be used to develop THz filter and slow-light devices.

Acknowledgements This work was supported by National Natural Science Foundation of China (Nos. 11674213, 61735010, 11574195, 11774220).

References

1. M. Tonouchi, Cutting-edge terahertz technology. *Nat. Photon.* **1**(2), 97–105 (2007)
2. H. Song, T. Nagatsuma, Present and future of terahertz communications. *Terahertz Sci. Technol. IEEE Trans.* **1**(1), 256–263 (2011)
3. W.L. Chan, K. Charan, D. Takhar, K.F. Kelly, R.G. Baraniuk, D.M. Mittleman, A single-pixel terahertz imaging system based on compressed sensing. *Appl. Phys. Lett.* **93**(12), 121105 (2008)
4. B. Ferguson, X.C. Zhang, Materials for terahertz science and technology. *Nat. Mater.* **1**(1), 26–33 (2002)
5. K.J. Boller, A. Imamoglu, S.E. Harris, Observation of electromagnetically induced transparency. *Phys. Rev. Lett.* **66**(20), 2593 (1991)
6. S. Zhang, D.A. Genov, Y. Wang, Plasmon-induced transparency in metamaterials. *Phys. Rev. Lett.* **101**(4), 047401 (2008)
7. D.R. Smith, J.B. Pendry, Metamaterials and negative refractive index. *Science* **305**(5685), 788–792 (2004)
8. J. Valentine, S. Zhang, T. Zentgraf, E. Ulinavila, D.A. Genov, G. Bartal, X. Zhang, Three-dimensional optical metamaterial with a negative refractive index. *Nature* **455**(7211), 376 (2008)
9. S. Zhang, Y.S. Park, J. Li, Negative refractive index in chiral metamaterials. *Phys. Rev. Lett.* **102**(2), 023901 (2009)
10. D.R. Smith, N. Kroll, Negative refractive index in left-handed materials. *Phys. Rev. Lett.* **85**(14), 2933 (2000)
11. T. Ergin, N. Stenger, P. Brenner, Three-dimensional invisibility cloak at optical wavelengths. *Science* **328**(5976), 337–339 (2010)
12. X. Ni, Z.J. Wong, M. Mrejen, An ultrathin invisibility skin cloak for visible light. *Science* **349**(6254), 1310–1314 (2015)
13. J.B. Pendry, Negative refraction makes a perfect lens. *Phys. Rev. Lett.* **85**(18), 3966–3969 (2000)
14. X. Zhang, Q. Li, W. Cao, J. Gu, R. Singh, Z. Tian, J. Han, W. Zhang, Polarization-independent plasmon-induced transparency in a fourfold symmetric terahertz metamaterial. *IEEE J. Sel. Top. Quantum Electron.* **19**(1), 8400707 (2013)
15. X. Liu, J. Gu, R. Singh, W. Zhang, Electromagnetically induced transparency in terahertz plasmonic metamaterials via dual excitation pathways of the dark mode. *Appl. Phys. Lett.* **100**(13), 131101 (2012)
16. N. Papanikolaou, V.A. Fedotov, N.I. Zheludev, Metamaterial analog of electromagnetically induced transparency. *Phys. Rev. Lett.* **101**(25), 253903 (2008)
17. X. Piao, S. Yu, N. Park, Control of Fano asymmetry in plasmon induced transparency and its application to plasmonic waveguide modulator. *Opt. Express* **20**(17), 18994–18999 (2012)
18. N. Liu, L. Langguth, T. Weiss, Plasmonic analogue of electromagnetically induced transparency at the Drude damping limit. *Nat. Mater.* **8**(9), 758 (2009)
19. N. Liu, T. Weiss, M. Mesch, Planar metamaterial analogue of electromagnetically induced transparency for plasmonic sensing. *Nano Lett.* **10**(4), 1103–1107 (2010)

20. M. Liu, Z. Tian, X. Zhang, Tailoring the plasmon-induced transparency resonances in terahertz metamaterials. *Opt. Express* **25**(17), 19844–19855 (2017)
21. K.M. Devi, A.K. Sarma, D.R. Chowdhury, Plasmon induced transparency effect through alternately coupled resonators in terahertz metamaterial. *Opt. Express* **25**(9), 10484–10493 (2017)
22. J. Gu, R. Singh, X. Liu, X. Zhang, Y. Ma, S. Zhang, S.A. Maier, Z. Tian, A.K. Azad, H.T. Chen, A.J. Taylor, J. Han, W. Zhang, Active control of electromagnetically induced transparency analogue in terahertz metamaterials. *Nat. Commun.* **3**, 1151 (2012)
23. P. Pitchappa, M. Manjappa, C.P. Ho, Metamaterials: Active control of electromagnetically induced transparency analog in terahertz MEMS metamaterial. *Adv. Opt. Mater.* **4**(4), 540 (2016)
24. R. Yahiaoui, M. Manjappa, Y.K. Srivastava, Active control and switching of broadband electromagnetically induced transparency in symmetric metadevices. *Appl. Phys. Lett.* **111**(2), 021101 (2017)
25. C. Zhang, J. Wu, B. Jin, B. Jin, X. Jia, L. Kang et al., Tunable electromagnetically induced transparency from a superconducting terahertz metamaterial. *Appl. Phys. Lett.* **110**(24), 241105 (2017)
26. J. Wu, B. Jin, J. Wan, Superconducting terahertz metamaterials mimicking electromagnetically induced transparency. *Appl. Phys. Lett.* **99**(16), 36 (2011)
27. X. Su, C. Ouyang, N. Xu, S. Tan, J. Gu, T. Zhen, J. Han, F. Yan, W. Zhang, Broadband terahertz transparency in a switchable metasurface. *IEEE Photon J.* **7**(1), 1–8 (2015)
28. X. Zhao, C. Yuan, L. Zhu, J. Yao, Graphene-based tunable terahertz plasmon-induced transparency metamaterial. *Nanoscale* **8**(33), 15273–15280 (2016)
29. H. Cheng, S. Chen, P. Yu, Dynamically tunable plasmonically induced transparency in periodically patterned graphene nanostrips. *Appl. Phys. Lett.* **103**(20), 36 (2013)
30. S. Xiao, T. Wang, T. Liu, X. Yan, Z. Li, C. Xu, Active modulation of electromagnetically induced transparency analogue in terahertz hybrid metal-graphene metamaterials. *Carbon* **126**, 271–278 (2018)
31. T. Liu, H. Wang, Y. Liu, L. Xiao, Z. Yi, C. Zhou, S. Xiao, Active manipulation of electromagnetically induced transparency in a terahertz hybrid metamaterial. *Opt. Commun.* **426**, 629–634 (2018)
32. T. Liu, H. Wang, Y. Liu, L. Xiao, C. Zhou, Y. Liu, C. Xu, S. Xiao, Independently tunable dual-spectral electromagnetically induced transparency in a terahertz metal-graphene metamaterial. *J. Phys. D Appl. Phys.* **51**(41), 415105 (2018)
33. S. Xiao, T. Wang, X. Jiang, X. Yan, L. Cheng, B. Wang, C. Xu, Strong interaction between graphene layer and Fano resonance in terahertz metamaterials. *J. Phys. D Appl. Phys.* **50**(19), 195101 (2017)
34. T. Liu, Z. Yi, S. Xiao, Active control of near-field coupling in a Terahertz metal-graphene metamaterial. *IEEE. Photon. Tech. Lett.* **29**(22), 1998–2001 (2017)
35. M. Manjappa, S.Y. Chiam, L. Cong, A. Bettiol, W. Zhang, R. Singh, Tailoring the slow light behavior in terahertz metasurfaces. *Appl. Phys. Lett.* **106**(18), 181101 (2015)
36. M. Mesch, T. Weiss, M. Schaferling, M. Hentschel, R.S. Hegde, H. Giessen, Highly sensitive refractive index sensors with plasmonic nanoantennas-utilization of optimal spectral detuning of Fano resonances. *ACS Sens.* **3**(5), 960–966 (2018)
37. T. Tan, Y.K. Srivastava, M. Manjappa, E. Plum, R. Singh, Lattice induced strong coupling and line narrowing of split resonances in metamaterials. *Appl. Phys. Lett.* **112**(20), 201111 (2018)
38. D. Liang, H. Zhang, J. Gu, Y. Li, Z. Tian, C. Ouyang, J. Han, W. Zhang, Plasmonic analog of electromagnetically induced transparency in stereo metamaterials. *IEEE J. Sel. Top. Quantum Electron.* **23**(4), 1–7 (2017)
39. M.F. Limonov, M.V. Rybin, A.N. Poddubny, Y.S. Kivshar, Fano resonances in photonics. *Nat. Photon.* **11**, 543–554 (2017)

Publisher's Note Springer Nature remains neutral with regard to jurisdictional claims in published maps and institutional affiliations.